ELSEVIER

Journal of Neuroscience Methods 158 (2006) 242–250

JOURNAL OF NEUROSCIENCE METHODS

www.elsevier.com/locate/jneumeth

A low temperature embedding and section registration strategy for 3D image reconstruction of the rat brain from autoradiographic sections

Arjan W. Simonetti [a,b], Vedat A. Elezi [a,b], Régine Farion [a,b], Grégoire Malandain [c], Christoph Segebarth [a,b], Chantal Rémy [a,b], Emmanuel L. Barbier [a,b,*]

[a] *INSERM, Unité mixte 594, Neuroimagerie Fonctionnelle et Métabolique, Centre Hospitalier Universitaire Pavillon B, BP217, F-38043 Grenoble Cedex 09, France*

[b] *Université Joseph Fourier, Grenoble F-38043 Cedex 09, France*

[c] *Epidaure team, INRIA, 2004 route des lucioles, BP 93, Sophia-Antipolis F-06 902 Cedex, France*

Received 24 April 2006; received in revised form 6 June 2006; accepted 7 June 2006

Abstract

In studies on animal models of human brain pathologies, three-dimensional reconstruction from histological sections is particularly useful when assessing the morphologic, functional and biochemical changes induced by pathology. It allows assessing lesion heterogeneity in planes different from the cutting plane and allows correlating the histology with images obtained in vivo, such as by means of magnetic resonance imaging. To create a 3D volume from autoradiographic sections with minimal distortion, both cryosectioning as well as section registration need to be optimal. This paper describes a strategy whereby four external fiducial markers are positioned outside the rat brain with the use of a low temperature brain embedding procedure. The fiducial markers proposed here can be rapidly added to any frozen tissue block with no impact on the subsequent histological operations. Since embedding is performed at a low temperature, no tissue degradation occurs due to sample heating. The markers enable robust and almost error free registration, even in the presence of missing sections and poor image quality. Furthermore, the markers may be used to partially correct for global distortions.

Keywords: Autoradiography; Histology; Matching; Marker; Cerebral blood flow; Alignment; Co-registration; Cryosections; External fiducial marker

1. Introduction

Cryosectioning techniques are used extensively to obtain unfixed sections of brain tissue for subsequent immunological, morphological, biochemical or autoradiographic analysis. While direct analysis of 2D histological sections is very useful, it may be of additional interest to digitally reconstruct a 3D histological volume (Nikou et al., 2003; Ourselin et al., 2001; Schormann and Zilles, 1998; Toga and Thompson, 2001). For this purpose, registration techniques are needed (Hill et al., 2001; Maintz and Viergever, 1998). Reconstruction of 3D histological volumes allows the investigation of morphologic, biochemical and functional changes in brain regions due to pathology. Furthermore, 3D reconstruction allows integration of information over multiple slices and it yields the possibility to extract information from an anatomical volume, which is intrinsically three-dimensional.

Since the introduction of non-invasive tomographic imaging modalities such as magnetic resonance imaging, computed tomography and positron tomography, there is also a great interest in spatially matching high resolution, ex vivo, histological volumes with lower resolution, in vivo, images to assess the relationship between measured signal, micro-anatomy and function of the brain (Humm et al., 2003; Mega et al., 1997). This comparison involves the registration of two 3D volumes, from which at least one has been obtained from a set of 2D sections (Malandain et al., 2004).

Quality of the 3D volume reconstructed from a set of 2D sections is highly dependent on the registration method applied and on the quality of the individual sections. In this study, the 2D brain sections were obtained from rats that had been injected a freely diffusible radioactive tracer into the blood stream to quantify local cerebral blood flow by means of a classical autoradiographic approach (Sakurada et al., 1978).

* Corresponding author at: INSERM, Université Joseph Fourier, Unité mixte 594, Neuroimagerie Fonctionnelle et Métabolique, Centre Hospitalier Universitaire Pavillon B, BP217, F-38043 Grenoble Cedex 09, France.
Tel.: +33 4 76 76 57 48; fax: +33 4 76 76 58 96.
E-mail address: emmanuel.barbier@ujf-grenoble.fr (E.L. Barbier).

0165-0270/$ – see front matter © 2006 Elsevier B.V. All rights reserved.
doi:10.1016/j.jneumeth.2006.06.004

Registration methods based on the use of intrinsic landmarks (Maintz and Viergever, 1998) are not satisfactory in the case of autoradiography due to the time lapse between animal sacrificing and brain freezing. This causes the images to be unsharp (broadening of the point spread function), and therefore it becomes difficult to find valid intrinsic markers. When images are registered sequentially with respect to the preceding one, and if the number of slices is large, a global volume distortion may occur due to error propagation (Hess et al., 1998; Nikou et al., 2003). A basic problem in image registration is that consecutive slices are naturally dissimilar, even in the absence of data corruption. Finally, the non-contiguous sampling of images induces global deformations due to the shape of the object (so-called "banana problem") (Malandain et al., 2004; Streicher et al., 1997). These registration difficulties can be avoided by using extrinsic markers, either inside or outside the tissue sample. Accurately positioning internal markers in frozen tissue is difficult and will induce tissue damage (Hess et al., 1998).

During cryosectioning, brain slices may be deformed due to tears and folds. Some sections are so strongly affected that they may have to be discarded, leading to missing data. Also, compression of the section may occur due to the pressure of the cutting blade. The eventual distortion is dependent on the cutting depth, the rigidity of the material and the operator's skill (Zarow et al., 2004). These difficulties could be partially avoided by embedding the brain before cutting.

Brain embedding provides the opportunity to add fiducial markers outside the organ, and thus to perform extrinsic registration without inducing tissue damage. Classical embedding methods, whether applied with or without external markers, are performed at room, or even at higher temperatures (Bjarkam et al., 2001; Sorensen et al., 2000; Streicher et al., 1997; Williams and Doyle, 1996). They cannot be applied to frozen tissues, in particular to autoradiographic sections that may not defrost during processing.

To reconstruct 3D autoradiography volumes from tumour bearing rat brains with minimal distortion due to sectioning and registration, we developed a low temperature embedding procedure that includes the placement of four external fiducial markers. The procedure was optimized to embed the frozen brain at the lowest temperature possible. This is of particular importance in studies where diffusible tracers are used. The fiducial markers are clearly visible at the corners of the sections eventually obtained. Their positions are readily identified following segmentation of the digitized sections. These positions may be used to calculate the rotation/translation matrices that optimally register the entire set of sections. Moreover, the proposed approach can be performed rapidly (within less than 30 min) and has no impact on the earlier or later stages of the histological protocol.

2. Materials and methods

2.1. Animal handling

All operative procedures and animal care strictly conformed to French government guidelines (licenses 380321, A3851610004 and B3851610003). A total of four adult male Wistar rats (299 ± 35 g) were used in this study. For tumour implantation, rats were anesthetized (400 mg/kg chloral hydrate) and placed on a stereotactic head holder. A scalp incision was performed along the median line. A 2.5-mm diameter burr hole was drilled in the skull 3.5 mm lateral to the bregma. The cell suspension (10^5 cells in 5 μl) was injected in 10 s into the right caudate nucleus, at a depth of 3.5 mm under the dura. The Hamilton syringe was slowly removed 1 min after the injection. The burr hole was plugged with Horsley wax and the scalp sutured. Three weeks after tumour implantation, rats were anesthetized (isoflurane 4%) and maintained under a mixture of isoflurane (1.5%), air and O_2 ($FiO_2 = 40\%$). Arterial and venous catheters were placed in the femoral vessels. Rectal temperature was maintained at $37.0 \pm 0.5\,^{\circ}C$ throughout the experiment with a feedback-controlled heating pad.

2.2. Autoradiography

Autoradiography was performed following the procedure described by Sakurada et al. (1978). In rats, approximately 30 μCi of iodo[^{14}C]antipyrine in 1.2 ml of normal saline was infused during 1 min via a femoral venous catheter. The infusion rate was steadily increased from 1 to 1.5 ml/min. At the end of infusion, the animal was decapitated. The brain was rapidly dissected out and frozen in liquid nitrogen.

2.3. Embedding strategy

For embedding and subsequent cryosectioning of the frozen brain, we used an aluminium container (Fig. 1). The latter was mounted on a support and consists of several parts: a chuck, a square tube made of two parts screwed together, a lid and four needles of 1 mm diameter and 31 mm of length. The chuck is 22 mm × 18 mm, and has a crossing grid pattern to optimize gripping of the embedded tissue block. The tube is 35 mm high and fits over the chuck. The lid and the chuck have four holes each (1 mm in diameter) positioned in the corners at 2.5 mm from the edges and a large hole in the middle. Each needle is therefore guided through two holes, one in the lid and one in the chuck. This ensure that, when inserted, the needles are perfectly perpendicular to the chuck, and therefore to the cutting plane. All parts are stored at $-25\,^{\circ}C$.

The following procedure is followed for brain embedding. The chuck is mounted on the support. At each corner of the chuck (2.5 mm from the sides) a hole of 1 mm in diameter makes it possible to mount plastic spacers (Ø 6 mm, 16 mm height). These spacers facilitate a more precise and reproducible placement of the brain (Fig. 1a) and ensure that the brain will be sufficiently separated from the needles at their insertion. The brain is glued onto the chuck with Neg-50® (Richard Allan Scientific) stored at $4\,^{\circ}C$ using a cooled pair of tweezers. The plastic spacers are then removed and the tube is placed over the chuck. The lid is then put in place and the needles are inserted into the four corner holes (Fig. 1b). All operations are performed inside a cryotome at $-25\,^{\circ}C$. Next, Neg-50® at $4\,^{\circ}C$ is poured quickly into the container through the central hole in the lid. To reach the

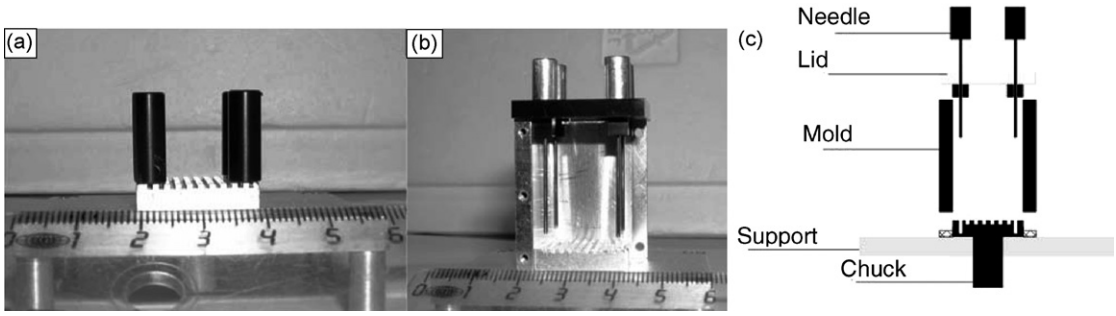

Fig. 1. (a) Side view of the container chuck with mounted spacers. The frozen rat brain can easily be mounted between the spacers. (b) The open container shows the position of the needles before Neg-50® is added. Normally, the container is closed and a rat brain is positioned inside before pouring the Neg-50®. (c) Drawings of all the pieces: needles (2 of 4), lid, mold, chuck and support.

bottom of the mold, a 5 cm long tube is connected to the bottle. Since all parts are cooled, the Neg-50® almost instantaneously becomes hard and maintains all parts of the mold together. After filling, the mold is rapidly removed from the support and cooled from the bottom in liquid nitrogen. Freezing of Neg-50® can be monitored easily as it turns from transparent to white. When ∼95% of the Neg-50® is frozen, the mold is removed from the liquid nitrogen. This avoids cracking of the block. The whole filling and freezing operation takes less than 60 s, thus avoiding inducing damage to the brain. After embedding, the temperature of the cryotome is raised to −8 °C. At this temperature the four needles can be pulled out gently, leaving perfectly parallel tracks. Lastly, the tube is removed by unscrewing the two parts.

To fill the four needle tracks, an acrylamide solution is used. Acrylamide has been found very useful for embedding (Bronson et al., 1991). Unfortunately, the solution and sample heat up during polymerization. While not applicable for frozen brain embedding, it may very well be used for markers. The marker solution is made of 950 μl of an 8% acrylamide solution mixed with 25 μl of Indian ink and 18 μl of iodo[14C]antipyrine solution (25 μCi/ml). The iodoantipyrine concentration in the solution is about the maximum concentration encountered in the brain sections. The Indian ink is added for enabling visual inspection of the markers. Other colorants can also be added if staining is needed. Three microliters of Ammonium Persulfate (APS, 30%) and 3 μl TEMED (*N*,*N*,*N*′,*N*′-tetramethylethylenediamine) are added before sucking up the marker solution with a 1 ml syringe equipped with a needle and a p10 catheter (outer diameter 0.61 mm). The catheter is pushed inside each track until the bottom of the chuk is reached. Then, gently some solution is pushed out of the syringe. All four tracks should be filled within 1 min after addition of the APS. The acrylamide solution is allowed to polymerize for 5 min, after which the block is stored at −80 °C.

2.4. Cryosectioning and digitization

After embedding, the block is cut into sections, 15 μm thick in the coronal orientation with respect to the rat brain. A LEICA CM 1900 cryotome was used. Since the chuck is constructed so as to fit in the cryotome, it has been ensured that the marker tracks are perpendicular to the cutting plane. Each sixth section is picked up on a glass histology slide, dried on a hot plate at 60 °C for at least 5 min., and subsequently placed in an X-ray cassette. Approximately, 170 sections are thus exposed to cover the whole rat brain. Autoradiographies are prepared with Kodak® single coated BIOMAX MR film. The exposure time is 6–7 days. After development of the film, each section is scanned with a 1200 dot per inch (dpi) resolution and 16 bit grey values on an Epson® 4870 Photo scanner with back lighting. This yields a dataset containing ∼170 × 1087 × 898 pixels per brain. The spatial homogeneity of the scanner was assessed and was found to vary within less than 5% over the whole scanner area.

2.5. Image preprocessing

Preprocessing and reconstruction software was developed using Matlab 6.5 and the Matlab image processing toolbox (The Mathworks Inc., Natick, MA, USA). The dataset (170 × 1087 × 898 pixels, 1200 dpi) was processed as it came out of the scanner (gray levels), prior to any blood flow quantification. The preprocessing starts by segmenting each image into five segments, four for the markers and one for the brain section (largest segment). Segmentation is performed by manual thresholding to obtain a black and white image. One threshold level was user-defined per dataset. Since the markers are circular, a 'disk shape' dilation with 20% of the marker diameter is applied. This is followed by hole filling and erosion of the segments. To obtain the marker locations in the image, the position of its centroid and the size of the marker segment are computed.

To double check whether the segments are really the markers, specific rules were verified such as theoretical positions (each segment in a different quadrant), sizes of the marker segments and distances between segments. If a segment does not comply with these rules, its assignment as marker is rejected. The registration method needs a minimum of two markers per section.

2.6. 3D reconstruction

All images are registered with respect to the four theoretical marker positions by a least squares regression in which all fiduciary markers are weighted equally (Goshtasby, 1986). More advanced methods based on Procrustes can be used as well (Goldszal et al., 1995; Hill et al., 2001). When less than two markers are found, the section is discarded. From the regression,

the optimal rotation, translation and scaling parameters can be calculated. No scaling factor is applied to the images, since this will have effects in both directions of the image. We observed in our data that the scaling needed was different between left–right and up–down directions (shear). Corrections for shear can be implemented, but are not at the moment.

2.7. Evaluation

We applied three different types of evaluation. First, the results were evaluated qualitatively by visual inspection following projection of the axial and sagittal sections of the 3D image. Especially, the markers provide visual insight into the quality of the registration. Second, the correlation between adjacent images was calculated before and after registration. Since the correlation of pixels outside the brain should not contribute to the interpretation, only the pixels inside the segmented brain area were used. It should be noted that a maximum correlation between images does not necessarily mean optimal alignment as two consecutive sections may exhibit significant differences in shape and morphology (in this study, sections are 90 μm apart). Third, our method was compared with an intensity-based method developed by Ourselin et al. (2001). This method assumes local similarities and tries to find the rigid transformation that matches a maximum of similar regions (block matching approach). As it relies on the brain data only, this method was applied to assess benefits from using markers. The block matching algorithm was used with five levels of pyramids, blocks of 4×4 and a trimmed least squares estimation procedure. The slice of reference was chosen by the operator as the first slice from the pile without artefacts (like fold or tear). The block matching approach was used because we wanted to compare a method that uses an embedding strategy with a method that does not. More precisely, we wanted to compare a method that uses advanced (mechanical) and time consuming preprocessing procedures together with relatively simple post-processing (segmentation, regression) with a method that uses relatively simple pre-processing together with advanced post-processing (block matching).

3. Results

Fig. 2 shows an example of the embedded brain. The markers (black due to Indian ink) and brain are clearly visible. The Neg-50® embeds the brain and the needles, despite the fact that it has been poured under cold conditions. The image in Fig. 3a shows a coronal autoradiograph from the middle region of the rat brain. A total of 175 sections were exposed for this experiment. The insufficient quality of 18 sections led us to discard them prior to digitization. In Fig. 3b, the ellipses represent the distribution of all centroid positions for marker one (top left) and three (bottom right): the centre of the ellipses corresponds to the mean of the centroid positions and the width of the ellipses indicates the standard deviation of the centroid positions in both directions. Mean standard deviation for all markers is 26 pixels (550 μm) in the horizontal direction, and 34 pixels (720 μm) in the vertical direction. This shows that it is possible to place most of the sections on the glass slides with minor variation, but that some will be positioned relatively far from the rest.

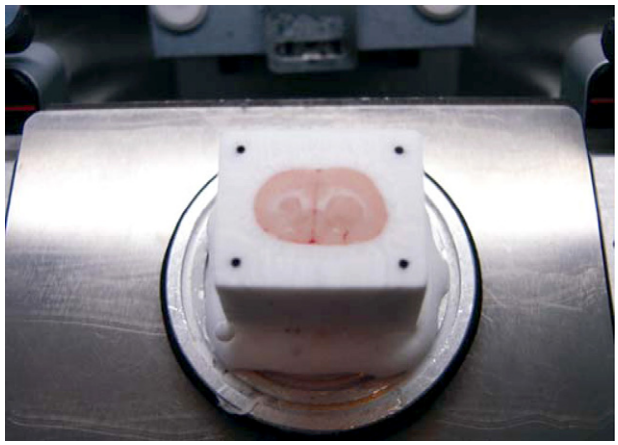

Fig. 2. An embedded brain mounted inside the cryotome. The four markers appear in black (Indian ink).

The result of segmentation is shown in Fig. 3c and d. In all cases, the algorithm automatically found the segment containing the brain. For seven slices not all markers were identified, but always a minimum of two. The ellipses again represent the distribution of all centroid positions, but now for the case after registration. The mean standard deviation for all markers has decreased to 5 pixels (106 μm) in the horizontal direction, and to 11 pixels (233 μm) in the vertical direction. The variance in the vertical direction is higher than in the horizontal direction. This indicates an irregular compression of the sections during sectioning. Due to the high contrast between marker and its surrounding, locating the markers is straightforward. In a number of cases the shape of the markers was not circular, as illustrated in Fig. 3e and f. This results in an incorrect positioning of the centroid. Since the registration is usually based on four centroids, this results in a small registration error. Note that the cutting artefacts observed within the brain in Fig. 3e have no impact on the slice registration since it only relies on the positions of the markers' centroids.

Fig. 4 shows images before registration, after registration using the method described here, and after registration using the intensity based method. Fig. 4a–c display the results before any registration. The coronal image (Fig. 4a) shows the same section as in Fig. 3a. The white dashes at the borders of the image indicate the position of the images reconstructed in the axial plane (Fig. 4b) and in the sagittal plane (Fig. 4c), respectively. A misalignment is clearly visible. The images that were discarded have been replaced by black images, so as to keep the relative position of all slices unchanged.

Fig. 4d–h display the results obtained with the registration method described here. Fig. 4d shows additional white dashes for the position of the axial and sagittal cross-sections for the marker tracks (Fig. 4f and h). These images are very important for evaluation of the registration. Fig. 4e and g show the registered axial and sagittal views of the brain, respectively.

Fig. 4i–l present the results obtained with the intensity based registration method (Ourselin et al., 2001). To keep the method

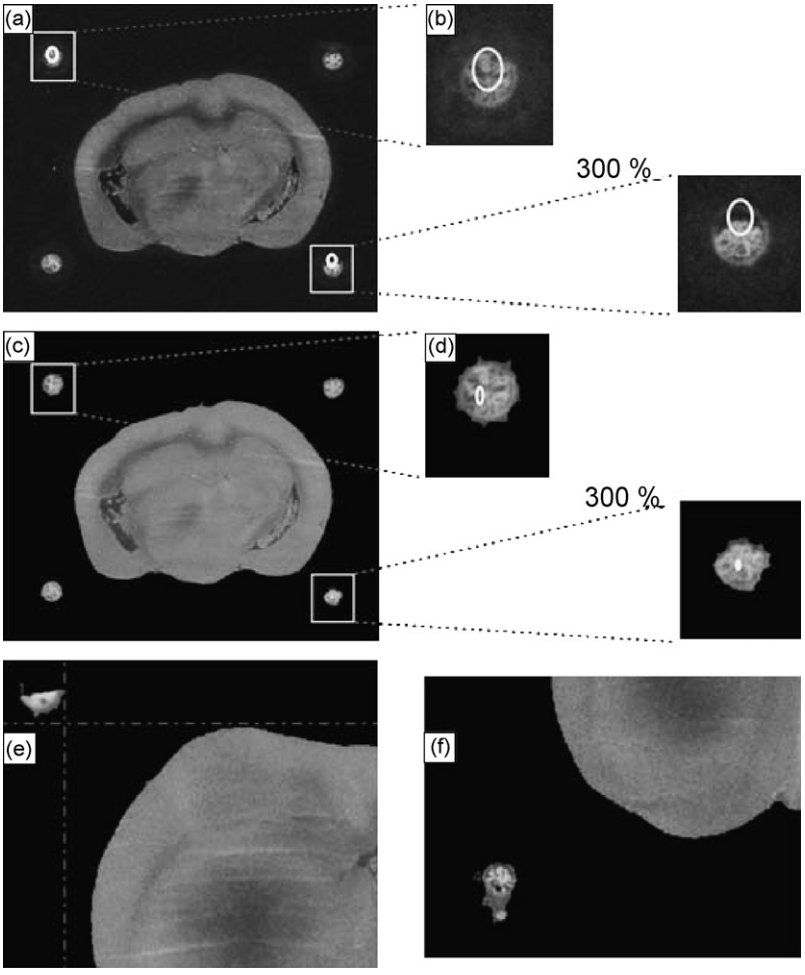

Fig. 3. (a) Example of a digitized autoradiography section and the surrounding fiducial markers. The ellipses show the distribution of centroid positions before registration (see text), (b) zoom on the rectangles delineated in (a), (c) the same section as in (a) but now segmented. The ellipses show the distribution of centroid positions after registration, (d) zoom on the rectangles delineated in (c), (e and f) zoom on two marker segments exhibiting artefacts (from different sections). Sometimes, the marker is partly missing, leading to segments like in (e). If the contrast of the marker with its surrounding is small, then the segmented area may be too large and irregular, like in (f).

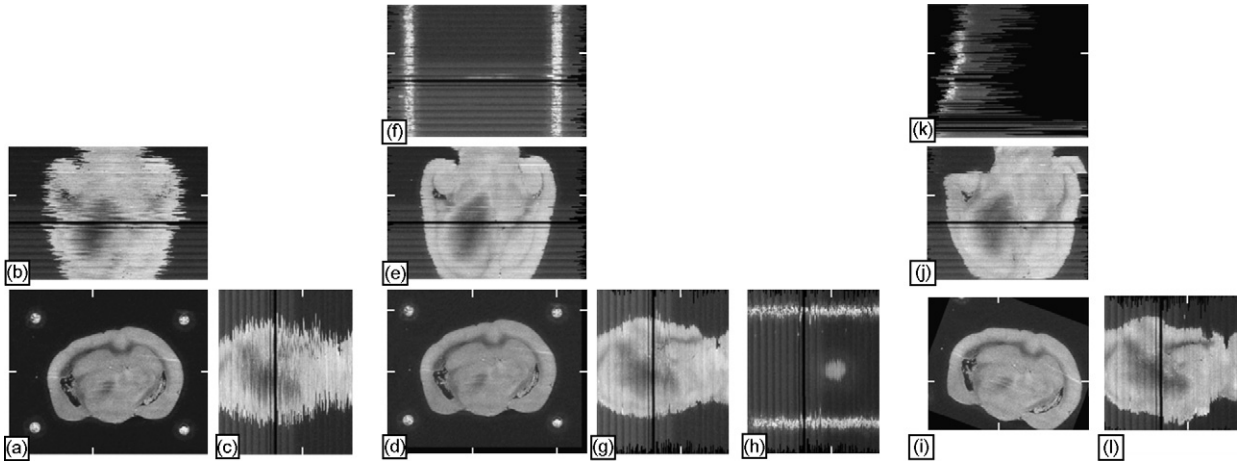

Fig. 4. Examples of reconstructed images from different directions for the unconnected data set (a–c), the 3D reconstruction method proposed in this paper (d–h) and the method proposed by Ourselin et al. (i–l). Images (a, d and i) represent coronal sections; images (c, g and l) represent sagittal sections; images (b, e and j) represent axial sections. When it is possible to obtain a single plane through the markers, this is represented (images f, h and k).

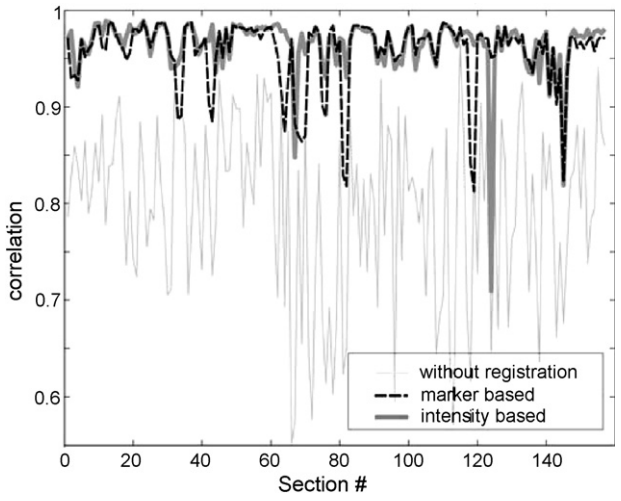

Fig. 5. Correlation values provide information about the quality of the registration and the number of misregistrations.

as robust as possible, only a subsection of the images was used to calculate the best rotation and translation values. The position of the cross-sections is again indicated by white dashes.

Fig. 5 shows the correlation between adjacent images before registration (grey), after registration using the proposed method (black-dashed thin line) and using the intensity based method (dark-grey thick line). Misregistrations are visible by peaks pointing downwards. Since in the proposed method each image is registered to a theoretic position, a misregistered image will lead to two adjacent points having a low correlation. In the intensity based method, a misregistered image will only lead to one point with a low correlation, but all sections after the misregistered one will be misregistered with respect to earlier images. The number of images that have low correlation (<0.9) with a neighbour is eight for the proposed method and three for the intensity based method. Thus, in this particular case, the number of misregistrations between consecutive images is lower for the intensity-based method.

Fig. 6a shows the rotation and translations applied for registration of the images using the proposed method. As expected, the values do not exhibit a dependence on the slice number. The rotation angles are always very low, and, with a few exceptions, translations do not exceed 50 pixels (1060 μm). Since each image is registered individually, no accumulating error is visible. For the intensity-based method, this does not seem to be the case (Fig. 6b). In particular, the rotation angle (solid line) shows a gradual increase which leads to a clockwise rotation (as it can be observed on Fig. 4i, taking Fig. 4a as a reference).

To illustrate the robustness of the registration method proposed here, the results obtained from the three other rats are shown in Fig. 7. Cross-sections with a maximum of the tumour area are shown. The images are very regular and tumour boundaries can be estimated very well.

4. Discussion

4.1. Embedding strategy

The embedding procedure protects the brain during sectioning and provides an excellent basis for the application of external markers without damaging the tissue. The low temperature during embedding ensures that the inner part of the brain does not defrost. It is difficult to assess whether the outer layer of the brain defrosts for a short period. Visual inspection did not reveal any damage to the brain border after embedding and sectioning. Therefore, we assume that embedding at low temperature is possible without damaging the brain itself. This is very important since most embedding strategies described in literature are performed at room temperature or even beyond (Bjarkam et al., 2001; Sorensen et al., 2000; Williams and Doyle, 1996).

Sectioning proves easier with embedding material than without. Bjarkam et al. (2001) and Zarow et al. (2004) have reported that embedding the sample minimizes the physical distortion usually associated with slicing and handling, especially for pathological material, allowing to cut soft and fragile tissue in thin, evenly sized, sections.

The use of internal fiducial markers has proven to provide excellent registration results (Hess et al., 1998). However, internal markers are difficult to place inside small frozen specimens, they damage the tissue, and they are sometimes difficult to identify. We therefore developed an approach using external markers (Streicher et al., 1997). After some practice, it becomes very easy to setup the markers, and in general, they stand sectioning very well. It happens that a marker partially disappears during the

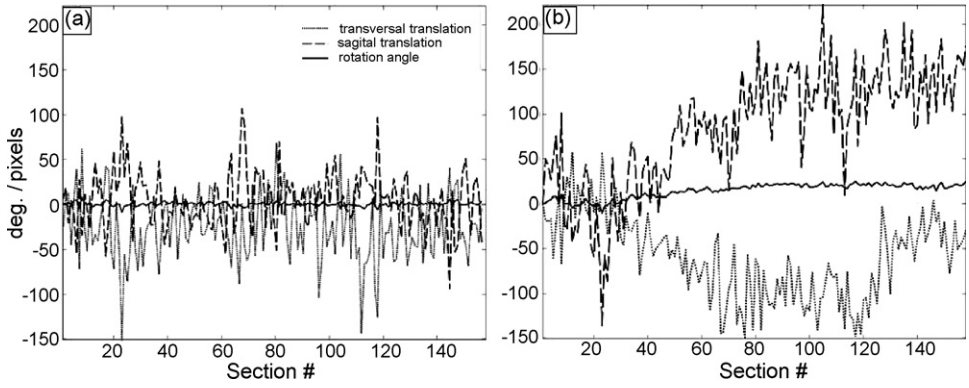

Fig. 6. Rotation angles and translations obtained for each image are displayed as a function of section number for the method proposed here (a) and for the intensity based method (b). With the latter method, the values displayed are cumulated rotations and translations with respect to the first section.

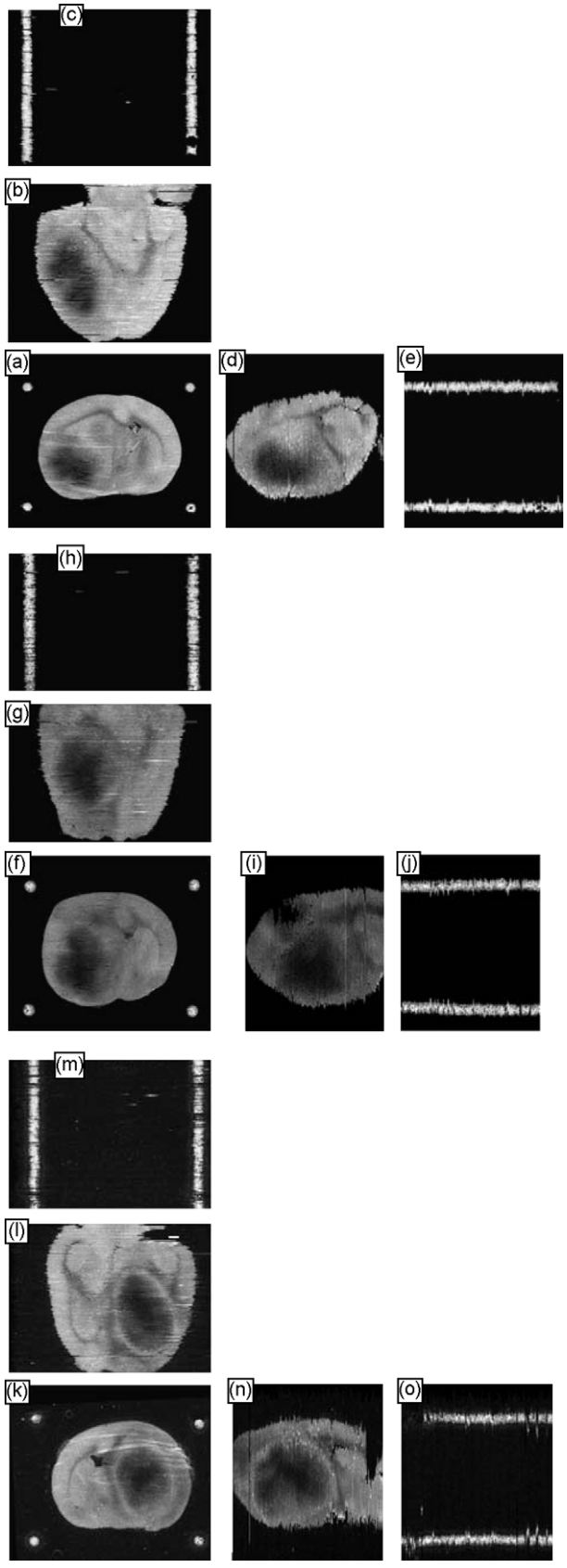

Fig. 7. Different views of the three other rat brains. Also cross-sections through the markers are shown (c, e, h, j, m and o).

cutting process (Fig. 3e) or that it gets deformed due to sectioning or incorrect segmentation (Fig. 3f). This may induce a bias in its centroid determination, and may cause a small registration error. Since the registration is based on four markers, the consequences are usually limited. The errors might be further reduced by using thinner markers and more robust segmentation algorithms. One possible strategy for improved segmentation could be to search for circular shapes with a specific diameter in the image to find the markers. Besides, we did not observe any deformation of the brain tissue relative to the markers (rigid hypothesis). Therefore, it was appropriate to rely on the centroid positions to register the brain tissue sections. Occasionally, section folding yields a rupture between the brain and the embedding. In this case, the section was discarded.

The contrast and type of the markers can be optimized for the particular histological procedure under consideration, e.g. a dose of radioactivity for autoradiography or a specific colour for histological staining. Neg-50® interferes neither with autoradiography nor with staining techniques and the acrylamide markers remain on the slide during staining.

4.2. Image preprocessing

The segmentation algorithm applied here is a classical one. Due to the high contrast to noise between markers or brain section and Neg-50®, segments follow the borders accurately. Most of the computation time is due to the segmentation, which is done with software developed in house. If more advanced methods or faster algorithms are used, computation time might decrease significantly. Here, we did not focus on computation time since this was not an issue.

4.3. 3D reconstruction

3D reconstruction provides excellent results if markers are used. Particularly the axial view (Fig. 4e) is very good. The imperfections of the sagittal view are due to the sectioning and not to the reconstruction procedure. During sectioning, the tissue is compressed due to the knife cutting the tissue (Gardella et al., 2003). This induces a slight wrinkling of the sections in one direction which is visible on the sagittal view as a compression of the section. The problem is less pronounced in Fig. 7e and j, and is likely affected by operator skills and cryotome brand and type. From the images showing the tracks (Figs. 4f, 4h, 7c, e, h, j, m and 7o) it appears that no global distortions occur. Registration is robust, even when one or two markers are absent. From Fig. 4i and k it may be noted that global deformation such as curvature, torsion or inclination of the vertical axis cannot be corrected for by an intensity based method (Malandain et al., 2004), and this is not indicated by the correlation between images that remains high (Fig. 5).

Reconstruction using markers has several advantages over other methods described in literature, such as principal-axes alignment, feature-based methods or intensity based techniques (Hibbard and Hawkins, 1988; Nikou et al., 2003; Ourselin et al., 2001; Rangarajan et al., 1997). The method is unbiased since it does not depend on the object of interest inside the block. It does

not rely upon the hypothesis of similarity of consecutive sections and can deal with missing images or low contrast images. This is especially important with autoradiography, since this procedure yields images with broad point spread function (absence of sharp edges). Another advantage of the proposed method is that errors do not accumulate, since each image is registered with respect to the marker locations of a reference image, or to prior defined marker locations. No manual input like landmarks are needed, which keeps the procedure as objective as possible.

The markers can furthermore be used to correct for several artifacts due to sectioning and subsequent imaging. Since the theoretical positions of the four makers are known, they could be used to rescale the image in the context of a linear deformation. For example, shear could be used to correct the digitized section for a compression along the cutting direction (assuming a linear compression). However, due to the distortion that may occur during cutting, all the sections that contain only two markers may not be included in the 3D reconstruction. Indeed, two markers will be sufficient for registration only if they are located in the opposite corners of the section. The sections with only two markers remaining on the same side should be discarded.

4.4. Evaluation

Markers can be readily added to any frozen tissue block with no impact on the subsequent histological operations. The tissue preparation last about 15 min. The registration procedure is relatively fast since no iterations are needed. With the setup used, the processing of one typical brain takes about half an hour. Since very little operator input is needed, the method is objective and the required processing time for the operator is only a couple of minutes. Our approach dedicated to frozen tissue samples differs from the approach proposed by Streicher et al. (1997) that requires room temperature manipulations of the sample and additional chemical treatments (like dehydration). As in our case, the positions of the markers are defined by the metallic mold, they can be thinner and better aligned (parallel trajectories) than holes drilled independently in the embedding material. Moreover, in our case, there is little risk of damaging the samples as no drilling is necessary. With our approach, there is a greater risk, however, to obtain incomplete markers (e.g. due to the presence of air bubbles) or non-circular markers (e.g. due to cutting artefacts or to diffusion of the marker's coloration into the embedding media during polymerization).

The registration performs very well as can been seen from Figs. 4 and 7. The axial as well as the sagittal views look very realistic, with little deformation. The markers are parallel throughout all slices and show a minimum of variance. There is no gradual shift of markers as in Fig. 4k.

Correlation of adjacent images is dramatically improved following registration with the method described here as well as with the intensity-based method. In general, the correlation between images for the intensity-based method is similar to the proposed method. The number of misregistrations (eight, compared to three with the intensity based method), represent 4.5% out of the total number of sections. Misregistrations are easy to track using correlation and images can be removed or registered manually without need for correction of all the following images. In the case of the intensity based method, misregistrations can be corrected by a change of the initial transformation parameters (Malandain et al., 2004). After visual inspection, in three of the eight misregistered images, the cryosectioning caused the section to be deformed, and therefore has shifted the markers. In the other cases, markers were missing or had been badly segmented. Numerous improvements to the proposed method can be though of in terms of image processing. Currently, the marker's position has been defined by its centroid. This could be improved by using a-priori knowledge about the marker's shape. For example, one could adjust the position of a 2D Gaussian profile the width of which would correspond to the actual marker's width. This approach could reduce the impact of noise (such as the one observed in Fig. 3) on the estimate of the marker's position and thereby improve the registration. One could also use an automated segmentation approach.

As anticipated, the method proposed outperforms the intensity-based method as it can compensate for curvature, torsion, or inclination of the vertical axis. This is important, particularly since small global transformations cannot be traced automatically. Therefore, they cannot be corrected for easily. Slice to slice misregistrations, in contrast, can be spotted automatically without difficulties and corrected for.

In conclusion, we developed a low temperature embedding method, which can be used to insert external markers outside of the rat brain before histological sectioning and 3D reconstruction. The brain can be easily and rapidly embedded with markers. The reconstruction is accurate and preserves the integrity of the brain. The embedding does not interfere with protocols like autoradiography and can be performed, in the absence of radioactivity, with different staining procedures. Embedding protects the brain during sectioning and the external markers can be used to perform additional image corrections such as linear stretching. The method has been applied here on autoradiography slices of the rat brain, providing an excellent high resolution 3D image. The method provides the possibility to match histology with magnetic resonance images in three-dimensions.

Acknowledgments

We gratefully acknowledge the French Ministry of Research for funding Dr. A.W. Simonetti, Dr. A. Nehlig for teaching us the autoradiography technique, and Dr. A.-S. Gauchez for enabling the use of radioactive material. The Inserm/UJF UM594 laboratory was the recipient of a grant "Imagerie du Petit Animal" (CNRS/INSERM/CEA).

References

Bjarkam CR, Pedersen M, Sorensen JC. New strategies for embedding, orientation and sectioning of small brain specimens enable direct correlation to MR-images, brain atlases, or use of unbiased stereology. J Neurosci Methods 2001;108:153–9.

Bronson DD, Bidmon HJ, Tomaschko KH, Stumpf WE. Novel applications of acrylamide for cryosectioning of isolated cells, tissues, and arthropods. J Histochem Cytochem 1991;39:1289–93.

Gardella D, Hatton WJ, Rind HB, Rosen GD, von Bartheld CS. Differential tissue shrinkage and compression in the *z*-axis: implications for optical dissector counting in vibratome-, plastic- and cryosections. J Neurosci Methods 2003;124:45–59.

Goldszal AF, Tretiak OJ, Hand PJ, Bhasin S, McEachron DL. Three-dimensional reconstruction of activated columns from 2-[14C]deoxy-D-glucose data. Neuroimage 1995;2:9–20.

Goshtasby A. Piecewise linear mapping functions for image registration. Pattern Recognit 1986;19:459–66.

Hess A, Lohmann K, Gundelfinger ED, Scheich H. A new method for reliable and efficient reconstruction of 3-dimensional images from autoradiographs of brain sections. J Neurosci Methods 1998;84:77–86.

Hibbard LS, Hawkins RA. Objective image alignment for three-dimensional reconstruction of digital autoradiograms. J Neurosci Methods 1988;26:55–74.

Hill DL, Batchelor PG, Holden M, Hawkes DJ. Medical image registration. Phys Med Biol 2001;46:R1–45.

Humm JL, Ballon D, Hu YC, Ruan S, Chui C, Tulipano PK, et al. A stereotactic method for the three-dimensional registration of multi-modality biologic images in animals: NMR, PET, histology, and autoradiography. Med Phys 2003;30:2303–14.

Maintz JB, Viergever MA. A survey of medical image registration. Med Image Anal 1998;2:1–36.

Malandain G, Bardinet E, Nelissen K, Vanduffel W. Fusion of autoradiographs with an MR volume using 2-D and 3-D linear transformations. Neuroimage 2004;23:111–27.

Mega MS, Chen SS, Thompson PM, Woods RP, Karaca TJ, Tiwari A, et al. Mapping histology to metabolism: coregistration of stained whole-brain sections to premortem PET in Alzheimer's disease. Neuroimage 1997;5:147–53.

Nikou C, Heitz F, Nehlig A, Namer IJ, Armspach JP. A robust statistics-based global energy function for the alignment of serially acquired autoradiographic sections. J Neurosci Methods 2003;124:93–102.

Ourselin S, Roche A, Subsol G, Pennec X, Ayache N. Reconstructing a 3D structure from serial histological sections. Image Vision Comput 2001;19:25–31.

Rangarajan A, Chui H, Mjolsness E, Pappu S, Davachi L, Goldman-Rakic P, et al. A robust point-matching algorithm for autoradiograph alignment. Med Image Anal 1997;1:379–98.

Sakurada O, Kennedy C, Jehle J, Brown JD, Carbin GL, Sokoloff L. Measurement of local cerebral blood flow with iodo [14C] antipyrine. Am J Physiol 1978;234:H59–66.

Schormann T, Zilles K. Three-dimensional linear and nonlinear transformations: an integration of light microscopical and MRI data. Hum Brain Mapp 1998;6:339–47.

Sorensen JC, Bjarkam CR, Danielsen EH, Simonsen CZ, Geneser FA. Oriented sectioning of irregular tissue blocks in relation to computerized scanning modalities: results from the domestic pig brain. J Neurosci Methods 2000;104:93–8.

Streicher J, Weninger WJ, Muller GB. External marker-based automatic congruencing: a new method of 3D reconstruction from serial sections. Anat Rec 1997;248:583–602.

Toga AW, Thompson PM. The role of image registration in brain mapping. Image Vision Comput 2001;19:3–24.

Williams BS, Doyle MD. An Internet atlas of mouse development. Comput Med Imaging Graph 1996;20:433–47.

Zarow C, Kim TS, Singh M, Chui HC. A standardized method for brain-cutting suitable for both stereology and MRI-brain co-registration. J Neurosci Methods 2004;139:209–15.